



Engineering the quantum measurement process for the persistent current qubit

T.P. Orlando^{a,*}, Lin Tian^a, D.S. Crankshaw^a, S. Lloyd^a, C.H. van der Wal^b, J.E. Mooij^b, F. Wilhelm^c

^a *Massachusetts Institute of Technology, 77 Mass. Ave., Cambridge, MA 02139, USA*

^b *Delft University of Technology, P.O. Box 5046, 2628 CJ Delft, The Netherlands*

^c *Ludwig-Maximilians-Universitaet, Theresienstr. 37, 80333 Munich, Germany*

Abstract

The SQUID used to measure the flux state of a superconducting flux-based qubit interacts with the qubit and transmits its environmental noise to the qubit, thus causing the relaxation and dephasing of the qubit state. The SQUID–qubit system is analyzed and the effect of the transmittal of environmental noise is calculated. The method presented can also be applied to other quantum systems. © 2001 Elsevier Science B.V. All rights reserved.

PACS: 03.67.Lx; 74.90.+n; 85.25.Dq; 85.25.Cp J

Keywords: Quantum bit; Quantum computing; Superconductive devices

1. Introduction—the qubit

Present schemes for the measurement of a single flux-based superconducting qubit usually employ a SQUID as the measurement meter [1–6]. The meter, however, is permanently coupled to the single qubit and becomes entangled with it. This coupling also allows a channel for the environment to interact indirectly with the qubit to cause decoherence. Therefore, a detailed analysis of the particular measurement scheme is necessary for engineering the decoherence to an acceptable level. In this paper we will analyze a persistent current qubit surrounded by a DC SQUID as the meter.

The method outlined here is applicable to other flux-based qubits and other schemes of measurements.

The persistent current qubit is a macroscopic quantum system which consists of a superconducting ring interrupted by three Josephson junctions [2].

When the external flux bias $\Phi_{\text{ext}} = f_{\text{ext}} \Phi_0$ is near $f_{\text{ext}} = 1/2$, the periodic potential of the qubit has two wells. These two lowest energy states correspond to a persistent current I_{pc} circulating in opposite directions, and these are the $|0\rangle$ and $|1\rangle$ states of the qubit. The qubit is represented symbolically in Fig. 1 as a ring with an up-arrow denoting the magnetic moment of the $|0\rangle$ state. L_{pc} is the self-inductance of the qubit loop, L_{SQ} is the geometric inductance of the DC SQUID, M is the mutual inductance. I_s is the circulating current in

* Corresponding author.

E-mail address: orlando@mit.edu (T.P. Orlando).

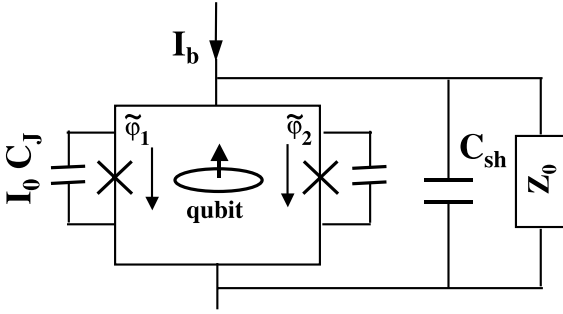


Fig. 1. The measuring circuit of the DC SQUID which surrounds the qubit. C_J and I_0 are the capacitance and critical current of each of the junctions, and $\tilde{\varphi}_i$ are the gauge-invariant phases of the junctions. The qubit is represented symbolically by a loop with an arrow indicating the magnetic moment of the $|0\rangle$ state. The SQUID is shunted by a capacitor C_{sh} and the environmental impedance $Z_0(\omega)$.

the DC SQUID and I_b is the bias current. For both loops, $L_i I_i \ll \Phi_0$.

A model Hamiltonian for these two states of the qubit is $H_q = (\epsilon_0)\sigma_z + (t_0/2)\sigma_x$. Here, $U_{\pm} = \pm \Phi_0 I_{pc}(f_{ext} - 1/2)$ is the potential energy of the upper (lower) state caused by the magnetic field for small self-inductance so that $\epsilon_0 = U_+ - U_- = 2\Phi_0 I_{pc}(f_{ext} - 1/2)$; and t_0 is the coupling energy due to tunneling. The corresponding energy difference ν between the two states is $\nu = (\epsilon_0^2 + t_0^2)^{1/2}$. Using an external oscillator, the energy level difference has been mapped out for the persistent current qubit [4] and also for the RF-SQUID qubit [5].

2. The meter

The state of the qubit adds or subtracts flux in the loop of the DC SQUID. Because the critical current I_c of the DC SQUID is modulated by the total flux in its loop, the state of the qubit can be inferred from the change ΔI_c .

To be more quantitative, we consider the Hamiltonian of the coupled systems. The DC SQUID has two Josephson junctions which have gauge-invariant phases $\tilde{\varphi}_1$ and $\tilde{\varphi}_2$ respectively. For convenience of discussion, we assume the two junctions are identical. When the self-inductance L_{SQ} and mutual inductance M of the SQUID are

considered, we have the flux quantization relation: $\tilde{\varphi}_1 - \tilde{\varphi}_2 = -2\pi(f_{ext} + L_{SQ}I_s/\Phi_0 + MI_{pc}/\Phi_0)$, where I_s is the circulating current in the DC SQUID. The Lagrangian of the SQUID is $L = T - U$, in terms of $\tilde{\varphi}_1$ and $\tilde{\varphi}_2$,

$$T = \frac{C_J}{2} \left(\frac{\Phi_0}{2\pi} \dot{\tilde{\varphi}}_1 \right)^2 + \frac{C_J}{2} \left(\frac{\Phi_0}{2\pi} \dot{\tilde{\varphi}}_2 \right)^2 + \frac{C_{sh}}{2} \left(\frac{\Phi_0}{4\pi} (\dot{\tilde{\varphi}}_1 + \dot{\tilde{\varphi}}_2) \right)^2, \quad (1)$$

$$U = -E_J^{SQ} \cos \tilde{\varphi}_1 - E_J^{SQ} \cos \tilde{\varphi}_2 + \frac{L_{SQ}}{2} I_s^2 - I_b \frac{\Phi_0}{4\pi} (\tilde{\varphi}_1 + \tilde{\varphi}_2)$$

where C_J is the junction capacitance, and C_{sh} is the shunt capacitance parallel to the SQUID. $E_J^{SQ} = I_0 \Phi_0 / (2\pi)$ is the Josephson energy of the junctions in the SQUID. The first three terms in the Lagrangian depend on the time derivatives of the phase variables and are the charging energies of the capacitances. U is the potential energy of the SQUID, including the Josephson energies of the junctions, the energy due to the self-inductance, and the work done by the bias current I_b .

The Hamiltonian of the qubit–SQUID system can be derived from the Lagrangian by adding the qubit Hamiltonian H_q to the total energy. We choose the independent variables of the SQUID to be: $\tilde{\varphi}_p = (\tilde{\varphi}_1 + \tilde{\varphi}_2)/2$ and $\tilde{\varphi}_m = (\tilde{\varphi}_1 - \tilde{\varphi}_2)/2$. $\tilde{\varphi}_p$ is the external variable that directly correlates with the ramping current I_b , and $\tilde{\varphi}_m$ is the inner variable that corresponds to the circulating current of the SQUID. $\tilde{\varphi}_m$ inductively couples with the qubit flux. The total Hamiltonian of the qubit–SQUID system is:

$$\begin{aligned} H_t &= H_q + H_{SQ} + H_{int}, \\ H_q &= \frac{\epsilon_0}{2} \sigma_z + \frac{t_0}{2} \sigma_x, \\ H_{SQ} &= \frac{P_p^2}{2m_p} + \frac{P_m^2}{2m_m} - 2E_J^{SQ} \cos \tilde{\varphi}_p \cos \tilde{\varphi}_m \\ &\quad + 2E_J^{SQ} \frac{(\tilde{\varphi}_m + \pi f_{ext})^2}{\beta_{SQ}} - I_b \frac{\Phi_0}{2\pi} \tilde{\varphi}_p, \\ H_{int} &= \frac{4\pi f_s E_J^{SQ}}{\beta_{SQ}} (\tilde{\varphi}_m + \pi f_{ext}) \sigma_z \end{aligned} \quad (2)$$

which includes the qubit Hamiltonian H_q , the SQUID Hamiltonian H_{SQ} under external flux f_{ext} ,

and the qubit–SQUID interaction H_{int} . P_p and P_m are the conjugate variables of the corresponding phases. $m_m = 2C_J(\Phi_0/2\pi)^2$ is the mass of the inner variable; $m_p = (C_{\text{sh}} + 2C_J)(\Phi_0/2\pi)^2$ is the mass of the external variable. For convenience we introduce $\beta_{\text{SQ}} = 2\pi L_{\text{SQ}}I_0/\Phi_0$ to represent the self-inductance.

Typical parameters of the experiments are: $E_J^{\text{SQ}} = 40$ GHz with $I_0 = 80$ nA, $C_J = 2$ fF, $C_{\text{sh}} = 5$ pF, $L_q = 10$, $L_{\text{SQ}} = 16$ pH and $M = 8$ pH. The circulating current of the qubit gives a flux of $f \approx 10^{-3}$ flux quanta, which is coupled to the SQUID by mutual inductance.

The mutual inductive coupling also changes the flux through the qubit. However, since the magnetic energy of the qubit states is linear near $f = 1/2$, the potential energies of the upper and lower states are $U_{\pm} = \pm\Phi_0 I_{\text{pc}}(f_{\text{ext}} + MI_s/\Phi_0 \pm L_q I_{\text{pc}}/\Phi_0 - 1/2)$ where L_q is the self-inductance of the qubit. Therefore, the energy difference is $\epsilon = U_+ - U_- = 2\Phi_0 I_{\text{pc}}(f_{\text{ext}} + MI_s/\Phi_0 - 1/2)$. However, $f_{\text{ext}} \gg MI_s/\Phi_0$ so that to lowest order, ϵ does not change; nevertheless, the mutual inductive coupling will be important when we consider it as the main channel through which environmental noise interacts with the qubit. Also to first order the tunneling does not change, so that H_q remains the same.

The current I_{sw} , at which the SQUID switches from the zero voltage state to the finite voltage state, is smaller than I_c due to thermal activation and quantum tunneling. What is measured experimentally then is a histogram of switching currents for a given applied flux as the bias current I_b is swept linearly in time. The circuitry which shunts the SQUID affects the statistics of I_{sw} [7–9]. An underdamped SQUID has $I_{\text{sw}} < I_c$ and the histograms are wide and require a number of repeated measurements for the needed resolution. A damped SQUID can give a narrow histogram at the expense of decoherence. Hence, a compromise is needed to damp the SQUID sufficiently to gain a fast, sensitive readout while maintaining a long coherence time. In this paper we will focus on underdamped SQUIDS as used in the recent experiments, but the method holds for damped SQUIDS also. The repetition frequency of the measurement of I_{sw} is limited by the bandwidth of

the low pass filters used for the measurements and by the read-out electronics. This limits the repetition frequency to the range of 10 kHz to 1 MHz. A more efficient readout may be realized by measuring the dynamical inductance of the SQUID [11].

3. Decoherence engineering

The relaxation and dephasing times may be found by solving the master equation for the reduced density in the spin–boson model [12,13]. The relaxation and dephasing times in terms of the spectral density of the effective environmental noise $J_{\text{eff}}(\omega)$ are

$$\frac{1}{\tau_r} = \frac{t_0^2}{2\omega_0^2} \left[J_{\text{eff}}(\omega) \coth \frac{\hbar\omega}{2k_B T} \right]_{\omega=\omega_0}, \quad (3)$$

$$\frac{1}{\tau_\phi} = \frac{1}{2\tau_r} + \frac{\epsilon_0^2}{\omega_0^2} \left[J_{\text{eff}}(\omega) \coth \frac{\hbar\omega}{2k_B T} \right]_{\omega \rightarrow 0}$$

where $\omega = \nu/\hbar$ is the frequency corresponding to the average energy difference of the qubit states.

The environmental spectral density function is calculated from the fluctuations in the energy levels of the qubit, $J_{\text{eff}} = \langle \delta\epsilon \delta\epsilon \rangle / \hbar^2$. Intuitively, the change in the energy level $\epsilon = 2\Phi_0 I_{\text{pc}}(f_{\text{ext}} + MI_s/\Phi_0 - 1/2)$ is $\delta\epsilon = 2I_{\text{pc}}M\delta I_s$, where we have assumed that the external bias field is constant and the main source of fluctuations is the Johnson noise acting through the circulating current in the SQUID. The bias current for the SQUID is $I_b = 2I_0 \cos \tilde{\varphi}_m \sin \tilde{\varphi}_p$ and the circulating current is $I_s = 2I_0 \sin \tilde{\varphi}_m \cos \tilde{\varphi}_p$. Let $\tilde{\varphi}_m \approx \pi f_{\text{ext}}$ so that

$$\frac{dI_s}{dt} = -2I_0 \sin(\pi f_{\text{ext}}) \sin \tilde{\varphi}_p \frac{2\pi}{\Phi_0} V \quad (4)$$

where $V = (\Phi_0/2\pi)d\tilde{\varphi}_p/dt$ is the voltage across the SQUID. Taking the Fourier transform of the above and using the definition of I_b , we have

$$\delta I_s(\omega) = i \frac{2\pi}{\omega\Phi_0} I_b \tan(\pi f_{\text{ext}}) \delta V(\omega). \quad (5)$$

The fluctuations in the voltage are given by the Johnson–Nyquist formula

$$\langle \delta V(\omega) \delta V(\omega) \rangle = \hbar\omega \text{Re}\{Z_t(\omega)\} \coth \frac{\hbar\omega}{2k_B T} \quad (6)$$

where $Z_t(\omega)$ is the total impedance seen by the SQUID, which in the case of Fig. 1 is a parallel combination of the environmental impedance and the capacitor C_{sh} . The spectral density function becomes

$$J_{\text{eff}}(\omega) = \frac{1}{\hbar\omega} \left(\frac{2\pi M I_{\text{pc}}}{\Phi_0} \right)^2 I_{\text{b}}^2 \times \tan^2(\pi f_{\text{ext}}) \text{Re}\{Z_t(\omega)\} \coth \frac{\hbar\omega}{2k_{\text{B}}T} \quad (7)$$

where $\tilde{\varphi}_{\text{m}} \approx \pi f_{\text{ext}}$.

A more detailed analysis [13] begins by linearizing the Hamiltonian, which was implicitly assumed in the more intuitive approach. After linearizing the potential energy near the energy minimum, the SQUID variables behave as harmonic oscillators interacting with each other, and the Hamiltonian becomes

$$H_t = H_{\text{q}} + \frac{P_{\text{m}}^2}{2m_{\text{m}}} + \frac{1}{2} m_{\text{m}} \omega_{\text{m}}^2 (\varphi_{\text{m}} + \delta\varphi_0 \sigma_z)^2 + \frac{P_{\text{p}}^2}{2m_{\text{p}}} + \frac{1}{2} m_{\text{p}} \omega_{\text{p}}^2 \varphi_{\text{p}}^2 + J_1 \varphi_{\text{m}} \varphi_{\text{p}}. \quad (8)$$

The phases $\varphi_{\text{m}} = \tilde{\varphi}_{\text{m}} - \tilde{\varphi}_{\text{m}}^0$ and $\varphi_{\text{p}} = \tilde{\varphi}_{\text{p}} - \tilde{\varphi}_{\text{p}}^0$ are the oscillator coordinates relative to the energy minimum ($\tilde{\varphi}_{\text{m}}^0, \tilde{\varphi}_{\text{p}}^0$). The inner oscillator frequency depends on the self-inductance of the SQUID, L_{SQ} , and the capacitance of the junctions C_{J} , as $\omega_{\text{m}} = \sqrt{2/L_{\text{SQ}}C_{\text{J}}}$. In the experiment, the self-inductance of the SQUID is weak with $\beta_L = 2\pi L_{\text{SQ}}I_0/\Phi_0 = 0.004$. Hence $\omega_{\text{m}} \approx 10^3$ GHz is higher than all the other relevant energies of the qubit–SQUID system. As a result, the inner oscillator is slaved to the qubit and follows the qubit’s dynamics even during qubit operation. The external oscillator frequency depends on the ramping current as $\omega_{\text{p}} = \omega_{\text{p}}^0 [1 - (I_{\text{b}}/I_{\text{c}})^2]^{1/4}$ where $\omega_{\text{p}}^0 = \sqrt{2\pi I_{\text{c}}/(C_{\text{sh}}\Phi_0)}$ is the oscillator frequency at zero current and I_{c} is the effective critical current of the SQUID under external frustration. Typical numbers are $\omega_{\text{p}}^0 = 1.3$ GHz and $\omega_{\text{p}} = 1.0$ GHz at $I_{\text{b}} = 0.8I_{\text{c}}$. As I_{b} increases the potential barrier decreases faster than ω_{p} , and the linearization will become invalid when I_{b} is close enough to the critical current. It can be shown that the harmonic oscillator approximation stays valid until $I_{\text{b}} \approx 0.95I_0$. However, in the present experiment with a linear ramp of I_{b} , the

SQUID usually switches to the finite voltage state before this current. In Eq. (8), the inner oscillator coordinate φ_{m} is offset by the qubit by $\pm\delta\varphi_0$ when $\sigma_z = \pm 1$. This offset originates from the inductive interaction between the qubit and the SQUID: $\delta\varphi_0 = \pi M I_{\text{pc}}/\Phi_0$. The J_1 term is the bilinear coupling between φ_{m} and φ_{p} at the potential energy minimum and is determined by the ramping current I_{b} . We have $J_1 = |\tan \tilde{\varphi}_{\text{m}}^0| I_{\text{b}} \Phi_0/2\pi$. When the ramping current is turned off, the J_1 coupling disappears, and φ_{m} and φ_{p} interact via a higher order term $\varphi_{\text{m}}\varphi_{\text{p}}^2$ which brings negligible entanglement with the qubit state.

Hence, we can divide the qubit–SQUID system into two parts: the measured system that includes the qubit and the inner oscillator of the SQUID; and the “meter” that is the external oscillator of the SQUID. The current ramping process is the system–meter entanglement process. When the SQUID switches, the meter variable escapes from the supercurrent branch to the finite voltage branch and a macroscopically distinguishable record is obtained; in the process, the coherence of the system is completely destroyed by quasiparticle excitations at the gap voltage. Note that the switching current in any given measurement is not perfectly correlated with the state of the qubit. In other words the measurement is not strictly speaking a von Neumann measurement, but rather a more general positive operator valued measurement [14].

The effect of the environmental noise is included by adding to the Hamiltonian a bath of oscillators which are coupled to the modes of the system. In this case we only include the coupling to the external φ_{p} modes of the SQUID as the major source of noise. The spectral density of the bath is described by the Johnson–Nyquist spectral density of $Z_t(\omega)$, the shunting impedance [15]. The problem can then be recast in terms of an effective bath that the qubit itself sees; that is, the inner and external SQUID oscillations are absorbed into an effective bath. The spectral density of this effective bath can be found from the generalized susceptibility of the qubit by writing the equations of motion for the linearized Hamiltonian and considering the variables as classical variables [16,17].

By treating the Hamiltonian classically, the resulting equations of motion describe the time

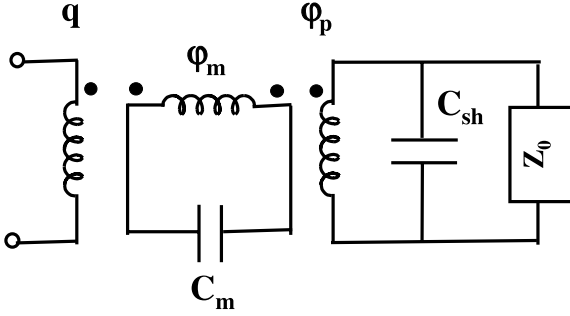


Fig. 2. Equivalent circuit of the linearized qubit-SQUID system. φ_m and φ_p are the two independent variables of a DC SQUID. φ_m corresponds to the circulating current of the SQUID, and φ_p couples with the ramping current of the SQUID. The capacitances of the inner oscillator loop and the external oscillator loop are $C_m = 2C_J$ and C_p , the shunt capacitance outside the SQUID. Flux of the three loops, $q = q_0\sigma_z$, φ_m , and φ_p , are chosen as independent variables in the calculation. Each of the inductances in the three loops interacts by mutual inductances as are indicated by the paired dots near the inductances.

evolution of the average of the quantum variables σ_z , φ_m , and φ_p . For the example in Fig. 1, the resulting linear equations can be represented by the equivalent circuit in Fig. 2 [13]. The reservoir of the SQUID has been modeled as an impedance $Z_0(\omega)$. The effective admittance Y_{eff} of this circuit is the inductance of qubit in parallel with a contribution from the outer circuits through the mutual inductive coupling with the inner oscillator. This contribution depends on the SQUID oscillator parameters and the impedance Z_0 . The current noise from this effective admittance is $J_{\text{eff}}(\omega) = (\hbar\omega/4e^2)\text{Re}[Y_{\text{eff}}]$. When $\omega_m \gg \omega_p, \omega$, we have:

$$J_{\text{eff}}(\omega) \approx \frac{(eI_b M I_{\text{pc}})^2}{C_{\text{sh}}^2 \hbar^3 R_{\text{sh}}} \frac{\omega}{(\omega^2 - \omega_p^2)^2 + (\omega/R_{\text{sh}} C_{\text{sh}})^2} \quad (9)$$

where C_{sh} is the SQUID shunt capacitance and the shunt impedance Z_0 is simplified as a resistor R_{sh} . At $\omega \approx \omega_0$, the noise is filtered by a factor of $(\omega_p/\omega)^4$. When $\omega \sim \omega_p$, a sharp Lorentzian peak appears in the spectrum that has a width of $(R_{\text{sh}} C_{\text{sh}})^{-1}$.

Once $J_{\text{eff}}(\omega)$ is known, the decoherence and relaxation times can be calculated from Eq. (3).

We use the experimental parameters of $C_{\text{sh}} = 5$ pF, $M = 8$ pH, $I_{\text{pc}} = 80$ nA and $I_b = 0.8I_c$, and we assume an environmental impedance of $R_{\text{sh}} = 100 \Omega$. At a temperature of 20 mK the derived decoherence time is then $\tau_\phi = 4 \mu\text{s}$ at $I_b = 0.8I_c$, and the relaxation time is $\tau_r = 0.3$ s. The decoherence time is shorter than the estimated intrinsic noise decoherence of 0.1 ms [18]; while the relaxation time is long enough so that it will not hinder the extraction of accurate information of the qubit states.

4. Summary

The DC SQUID decoheres the qubit during the measurement, when the bias current of the SQUID is ramped up to measure the qubit's state. This means that while the SQUID's bias current is zero, it does not contribute to the decoherence of the qubit, and thus it does not degrade the Q (the number of operations which can be performed prior to qubit decoherence). Assuming that the operations have been completed, the only consideration required is whether the SQUID's bias current can be ramped to the switching point before the qubit can relax to its ground state, $t_{\text{ramp}} < \tau_r$. In the recent qubit experiments [4], however, excitations are applied to the qubit simultaneous to the ramping of the SQUID's current. This results in the application of the SQUID's dephasing at the same time as the logical operation, resulting in the short dephasing time observed. Note that this technique for calculating the decoherence can be applied to other circuits, some of which continuously couple to the qubit.

Similar analyses have been done for a shunting circuit which includes a resistor [10,19] and the coupling of an external driving circuit to this qubit, both by an external oscillator [10,19] and an on-chip oscillator [20].

Acknowledgements

The work at MIT is supported by AFOSR grant F49620-01-1-0457 funded under the Department of Defense University Research Initia-

tive on Nanotechnology (DURINT) program and by the ARDA, the Dutch Foundation for Fundamental Research on Matter (FOM) and the European TMR Research network on superconducting nanocircuits (SUPNAN). Work on type-II quantum computing at MIT is supported by the AFOSR. The authors would like to thank M. Grifoni, Daniel Nakada, Alexander ter Haar, and C.J.P.M. Harmans for helpful discussions.

References

- [1] M.F. Bocko, A.M. Herr, M.F. Feldman, *IEEE Trans. Appl. Supercond.* 7 (1997) 3638.
- [2] J.E. Mooij, T.P. Orlando, L. Tian, C.H. van der Wal, L. Levitov, S. Lloyd, J.J. Mazo, *Science* 285 (1999) 1036.
- [3] T.P. Orlando, J.E. Mooij, L. Tian, C.H. van der Wal, L.S. Levitov, S. Lloyd, J.J. Mazo, *Phys. Rev. B* 60 (1999) 15398.
- [4] C.H. van der Wal, A.C.J. ter Haar, F.K. Wilhelm, R.N. Schouten, C.J.P.M. Harmans, T.P. Orlando, S. Lloyd, J.E. Mooij, *Science* 290 (2000) 773.
- [5] J.R. Friedman, V. Patel, W. Chen, S.K. Tolpygo, J.E. Lukens, *Nature* 406 (2000) 43.
- [6] P. Carelli, M.G. Castellano, F. Chiarello, C. Cosmelli, R. Leoni, G. Torrioli, *IEEE Trans. Appl. Supercond.* 11 (2001) 210.
- [7] J. Clarke, A.N. Cleland, M.H. Devoret, D. Esteve, J. Martinis, *Science* 239 (1988) 992.
- [8] D. Vion, M. Götze, P. Joyez, P.J.D. Esteve, M.H. Devoret, *Phys. Rev. Lett.* 77 (1997) 3435.
- [9] P. Joyez, D. Vion, M. Götze, M.H. Devoret, D. Esteve, *J. Supercond.* 12 (1999) 757.
- [10] C.H. van der Wal, Quantum superpositions of persistent current qubits, Ph.D. thesis, Technical University of Delft, The Netherlands, 2001.
- [11] C. Harmans, private communications.
- [12] M. Grifoni, E. Paladino, U. Weiss, *Euro. Phys. J. B* 10 (1999) 719.
- [13] L. Tian, S. Lloyd, T.P. Orlando, preprint, 2001.
- [14] A. Peres, *Quantum theory: Concepts and Methods*, Kluwer, The Netherlands, 1993.
- [15] M.H. Devoret, in: S. Reynaud, E. Giacobino, J. Zinn-Justin (Eds.), *Quantum Fluctuations*, Elsevier, Amsterdam, 1997.
- [16] A.J. Leggett, *Phys. Rev. Lett.* 30 (1984) 1208.
- [17] A. Garg, J.N. Onuchic, V. Ambegaokar, *J. Chem. Phys.* 83 (9) (1985) 4491.
- [18] L. Tian, L. Levitov, C.H. van der Wal, J.E. Mooij, T.P. Orlando, S. Lloyd, C.J.P.M. Harmans, J.J. Mazo, in: I.O. Kulik, R. Ellialoglu (Eds.), *Quantum Mesoscopic Phenomena and Mesoscopic Devices in Microelectronics*, Kluwer, The Netherlands, 2000.
- [19] C.H. van der Wal et al., preprint, 2001.
- [20] D.S. Crankshaw, E. Trías, T.P. Orlando, *IEEE Trans. Appl. Supercond.* 11 (2001) 1223.